

Memorandum M-2412

Page 1 of 30

Division 6 - Lincoln Laboratory  
Massachusetts Institute of Technology  
Cambridge 39, Massachusetts

SUBJECT: AN ANALYTICAL REVIEW OF NEÉL'S MOLECULAR FIELD THEORY OF FERRI- AND ANTIFERROMAGNETISM

To: D. R. Brown

From: Arthur L. Loeb

Date: September 16, 1953

Abstract: Néel's molecular field model of ferrimagnetism is reviewed and it is shown how the magnetization below the Curie point can be calculated as a function of temperature using susceptibility data obtained above the Curie temperature. While neither Néel's fundamental concepts nor his conclusions have been altered, his methods have been modified in order to obtain a clearer understanding of his results.

#### A. Introduction

This review is based on a paper by Néel,<sup>1</sup> and is written because it is felt that his presentation could be clarified by a reorganization of the material, a reduction in the number of fundamental concepts necessary for the derivations, and a reduction in the amount of quantitative material where only qualitative conclusions are drawn. Two secondary sources have been used: particularly for the treatment above and at the Curie point, the author is indebted to a Memorandum (31 July, 1952) by J. S. Smart and Louis N. Howard of the U. S. Naval Ordnance Laboratory, while for the ferrimagnetic region a great deal of material is drawn from the Seminar Notes on Magnetism (1952-53) by Arthur L. Loeb and Norman Menyuk of the Digital Computer Laboratory at MIT.

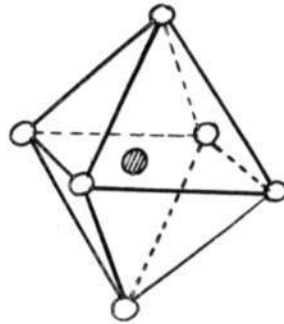
The following topics from Néel's theory are presented here:

- A. Introduction; ferrites and the spinel structure.
- B. The molecular field and the magnetic equation of state.
- C. The susceptibility of ferrimagnetic materials above the Curie temperature.
- D. The Curie temperature; spontaneous magnetization.
- E. Magnetization at and near the absolute zero.
- F. Antiferromagnetism.

---

1. Annales de Physique 3, (Mars.-Avril 1948), pp. 137-198.

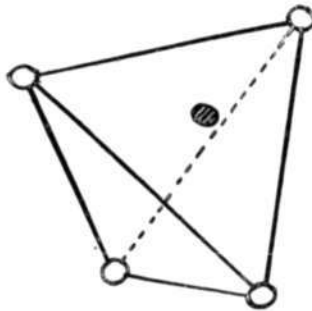
Ferrites frequently crystallize as spinels, which consist of a face centered cubic oxygen lattice with metal ions distributed over the tetrahedral (A-) and octahedral (B-) sites in between. (See Figures 1 and 2)



In spinel lattice

- - Oxygen atoms
- - Trivalent metallic ion in normal spinel structure
- ⊙ - Trivalent or divalent metallic ion in inverse spinel structure

Figure 1: Octahedron Configuration



In spinel lattice

- - Oxygen atoms
- - Divalent metallic ion in normal spinel structure
- ⊙ - Trivalent metallic ion in inverse spinel structure

Figure 2: Tetrahedron Configuration

Ferrites have the general chemical formula  $MO.Fe_2O_3$ , where M represents any divalent metal. Divalent metal ions are generally larger than trivalent ones and therefore tend to occupy tetrahedral sites, which are more spacious. In this case, the structure is called normal spinel. When half of the trivalent ions occupy tetrahedral sites and the divalent ions as well as half of the trivalent ions occupy octahedral sites, the structure is called inverse spinel. In general, the distribution of metal ions is described by a parameter  $\lambda$ , which defines the fraction of trivalent ions in the tetrahedral sites. The fraction of trivalent ions in the octahedral sites is called  $\mu$ , where  $\mu = 1 - \lambda$ . Generally the tetrahedral and octahedral sites contain the amounts of ions per molecule of ferrites shown in Table I.

Ions	Tetrahedral	Octahedral
M	$1 - 2\lambda \approx \mu - \lambda$	$2\lambda$
Fe	$2\lambda$	$2(1 - \lambda) \approx 2\mu$

Table I: Distribution of ions between A and B in a spinel expressed in number of ions per spinel molecule

For normal spinels  $\lambda = 0$ ,  $\mu = 1$ ; for inverse spinels  $\lambda = \mu = 0.5$ . Thus  $\lambda \leq \mu$ .

B. The Molecule Field and the "Equations of State"

Néel's paper<sup>1</sup> is mainly concerned with materials in which M is nonmagnetic. The magnetic properties of the ferrites then depend on the interaction between the  $Fe^{+3}$  ions distributed over the tetra- and octahedral sites. This interaction has its origin in the various quantum mechanical exchange energies between different  $Fe^{+3}$  ions, but can be described by molecular fields.

The exchange energy between two ions P and Q with resultant spins  $\vec{S}_P$  and  $\vec{S}_Q$  (in units of  $\hbar$ ) is given by Equation 1:

$$W_{pq} = -2J_{pq} \vec{S}_P \cdot \vec{S}_Q \quad \text{where } J_{pq} \text{ is the exchange integral} \quad \text{(Equ. 1)}$$

$W_{pq}$  is the exchange energy

When ion P is considered in the "molecular field" associated with the exchange interactions with all Q ions,  $\vec{S}_Q$  can be replaced by its mean value  $\vec{S}_Q = \frac{I_Q}{Ng\mu_B}$  where  $I_Q$  is the total magnetization of the Q ions, N the number of Q ions, g the Lande factor, and  $\mu_B$  the Bohr magneton.

The magnetic moment of ion P equals  $g\mu_B \vec{S}_P$ . The energy  $W_{pq}$  given by Equation 1 has the same value as that of P ion in a magnetic field  $U_{pq} I_Q$  where  $U_{pq}$  is given by Equation 2:

$$U_{pq} = \frac{2J_{pq}}{Ng\mu_B} \quad \text{(Equ. 2)}$$

The behavior of the  $Fe^{+3}$  ions in spinels may therefore be described by fictitious magnetic fields of the form  $\mu_{pq} I_q$ , which are called molecular fields. The molecular field due to Q ions is thus proportional to the magnetization of the Q ions, and is either parallel or antiparallel to this magnetization, depending on the sign of the molecular field coefficient  $U_{pq}$ .

When an  $Fe^{+3}$  ion in a tetrahedral site (an "A ion") is surrounded by  $Z_{aa}$  other A ions and by  $Z_{ab}$   $Fe^{+3}$  ions in octahedral sites ("B ions"), the molecular field acting on an A ion is given by Equation 3:

$$\vec{h}_a = Z_{aa} U_{aa} \vec{I}_a + Z_{ab} U_{ab} \vec{I}_b. \quad (\text{Equ. 3})$$

Similarly the molecular field acting on a B ion is given by Equation 4:

$$\vec{h}_b = Z_{ba} U_{ba} \vec{I}_a + Z_{bb} U_{bb} \vec{I}_b. \quad (\text{Equ. 4})$$

It can be shown quantummechanically that  $U_{ab} = U_{ba}$ . Per molecule of spinel there are one tetra and two octahedral sites. From Table I it is concluded that there are  $2\lambda$  A ions per A site, and  $\mu$  B ions per B site. In the spinel structure each A site has four A sites and twelve B sites as immediate neighbors, hence  $8\lambda$  A ions and  $12\mu$  B ions

$$\therefore Z_{aa} = 8\lambda, \quad Z_{ab} = 12\mu.$$

Since a B site is surrounded by six A sites and six B sites,

$$Z_{ab} = 12\lambda, \quad Z_{bb} = 6\mu.$$

Substitution in Equations (3) and (4) produces:

$$\vec{h}_a = 8\lambda U_{aa} \vec{I}_a + 12\mu U_{ab} \vec{I}_b. \quad (\text{Equ. 5})$$

$$\vec{h}_b = 12\lambda U_{ba} \vec{I}_a + 6\mu U_{bb} \vec{I}_b. \quad (\text{Equ. 6})$$

Two antiparallel unit vectors  $\hat{a}$  and  $\hat{b}$  are defined so that  $\vec{I}_a = I_a \hat{a}$  and  $\vec{I}_b = I_b \hat{b}$ . For ferrimagnetic materials  $I_a$  and  $I_b$  are positive, so that

$\vec{I}_a$  and  $\vec{I}_b$  are antiparallel. The vectors  $\hat{a}$  and  $\hat{b}$  have the following properties:

$$\hat{a} + \hat{b} = 0 \quad (\text{Equ. 7})$$

$$\hat{a} \cdot \hat{b} = -1 \quad (\text{Equ. 8})$$

The total magnetization is given by

$$\vec{I} = \lambda \vec{I}_a + \mu \vec{I}_b \quad (\text{Equ. 9})$$

$$\therefore \hat{a} \cdot \vec{I} = \lambda I_a - \mu I_b$$

$$\hat{b} \cdot \vec{I} = -\lambda I_a + \mu I_b$$

The absolute magnitude of the magnetization and its direction are then given by:

$$\begin{aligned} \vec{I} \text{ parallel to } \hat{a}, I &= \lambda I_a - I_b \text{ if } \lambda I_a > \mu I_b \\ \vec{I} \text{ parallel to } \hat{b}, I &= \mu I_b - \lambda I_a \text{ if } \mu I_b > \lambda I_a \end{aligned} \quad (\text{Equ. 9a})$$

Multiplying equation 5 by  $\hat{a}$  and Equation 6 by  $\hat{b}$  gives:

$$h_a \equiv \hat{a} \cdot \vec{h}_a = 8 \lambda U_{aa} I_a - 12 \mu U_{ab} I_b \quad (\text{Equ. 10})$$

$$h_b \equiv \hat{b} \cdot \vec{h}_b = 12 \lambda U_{ba} I_a - 6 \mu U_{bb} I_b \quad (\text{Equ. 11})$$

Define  $n \equiv |U_{ab}| = |U_{ba}|$ . Then if  $U_{ab} > 0$ ,  $n = U_{ab}$ , while when  $U_{ab} < 0$ ,  $n = -U_{ab}$ . The latter case corresponds to an interaction between A and B ions that tends to orient their magnetic dipoles antiparallel, while the former corresponds to a tendency to parallel orientation. This discussion is limited to the case  $U_{ab} < 0$ , which is of interest in ferromagnetism.

Defining further  $\alpha = 8 \frac{U_{aa}}{|U_{ab}|}$  and  $\beta = 6 \frac{U_{bb}}{|U_{ab}|}$  transforms Equation (10) and (11) into Equation (12) and (13):

$$h_a = n(\alpha \lambda I_a + \mu I_b) \quad (\text{Equ. 12})$$

$$h_b = n(\beta \mu I_b + \lambda I_a) \quad (\text{Equ. 13})$$

Equations (12) and (13) relate the molecular fields acting on A and B sites to the magnetization of these sites. Conversely an expression exists relating magnetization to magnetic field:

$$I = MB_j(z)$$

$$B_j(z) = \frac{2j+1}{2j} \coth \frac{2j+1}{2j} z = \frac{1}{2j} \coth \frac{z}{2j} \quad (\text{Equ. 9})$$

$$z = \frac{MH}{RT}$$

where M = molar magnetization in a magnetic field at the absolute zero of temperature

H = magnetic field

R = gas constant

j = total angular momentum quantum number

Thus if an external field  $H_o$  is imposed on the system, the following four equations relate the magnetizations and molecular fields at the A and the B sites:

$$h_a = n(\alpha \lambda I_a + \mu I_b) \quad (\text{Equ. 12})$$

$$h_b = n(\beta \mu I_b + \lambda I_a) \quad (\text{Equ. 13})$$

$$\vec{I}_a = M B_j \left[ \frac{M}{RT} (\vec{H}_o + \vec{h}_a) \right] \quad (\text{Equ. 14})$$

$$\vec{I}_b = M B_j \left[ \frac{M}{RT} (\vec{H}_o + \vec{h}_b) \right] \quad (\text{Equ. 15})$$

These four equations are called the magnetic equations of state; when they are solved the magnetization, molecular fields and susceptibility are known for any temperature and any external field. As an exact solution is very difficult to obtain, approximations are used for the various cases discussed below.

### C. Susceptibility above Curie Temperature

At high temperatures and in moderate fields the following expansion can be substituted into Equation (9):

$$\coth x = \frac{1}{x} + \frac{x}{3} + \dots$$

$$\therefore B(z) = \frac{j+1}{3j} z.$$

Thus Equations (14) and (15) can be written as follows:

$$\vec{I}_a - \frac{(j+1)M}{3jRT} \vec{h}_a = \frac{j+1}{3jRT} M \vec{H}_o \quad (\text{Equ. 16})$$

$$\vec{I}_b - \frac{(j+1)M}{3jRT} \vec{h}_b = \frac{j+1}{3jRT} M \vec{H}_o \quad (\text{Equ. 17})$$

Multiplying Equation (12) by  $\hat{a}$  and Equation (13) by  $\hat{b}$  produces:

$$I_a - \frac{(j+1)M}{3jRT} h_a = \frac{j+1}{3jRT} M \hat{a} \cdot \vec{H}_o$$

$$I_b - \frac{(j+1)M}{3jRT} h_b = \frac{j+1}{3jRT} M \hat{b} \cdot \vec{H}_o$$

Substituting Equation (12) and (13) gives:

$$I_a - \frac{nC_j}{T} (\alpha \lambda I_a + \mu I_b) = \frac{C_j}{T} \hat{a} \cdot \vec{H}_o \quad (\text{Equ. 18})$$

$$I_b - \frac{nC_j}{T} (\beta \mu I_b + \lambda I_a) = \frac{C_j}{T} \hat{b} \cdot \vec{H}_o \quad (\text{Equ. 19})$$

Therefore

$$(1 - \frac{nC_j}{T} \alpha \lambda) I_a - \frac{nC_j}{T} \mu I_b = \frac{C_j}{T} \hat{a} \cdot \vec{H}_o \quad (\text{Equ. 20})$$

$$-\frac{nC_j}{T} \lambda I_a + (1 - \frac{nC_j}{T} \beta \mu) I_b = \frac{C_j}{T} \hat{b} \cdot \vec{H}_o \quad (\text{Equ. 21})$$

These are solved to give:

$$I_a = \frac{\frac{C_j \hat{a} \cdot \vec{H}_o}{T} \left(1 - \frac{nC_j \beta \mu}{T}\right) + \left(\frac{nC_j}{T}\right)^2 \frac{\mu}{n} \hat{b} \cdot \vec{H}_o}{1 - \frac{nC_j}{T} (\alpha \lambda + \beta \mu) + \left(\frac{nC_j}{T}\right)^2 \lambda \mu (\alpha \beta - 1)}$$

$$I_b = \frac{\frac{C_j \hat{b} \cdot \vec{H}_o}{T} \left(1 - \frac{nC_j \alpha \lambda}{T}\right) + \left(\frac{nC_j}{T}\right)^2 \frac{\lambda}{n} \hat{a} \cdot \vec{H}_o}{1 - \frac{nC_j}{T} (\alpha \lambda + \beta \mu) + \left(\frac{nC_j}{T}\right)^2 \lambda \mu (\alpha \beta - 1)} \quad (\text{Equ. 22})$$

Therefore

$$I = \left| \frac{\frac{C_j}{T} \left\{ 1 - \frac{n C_j}{T} \lambda \mu (2 + \alpha + \beta) \right\}}{1 - \frac{n C_j}{T} (\alpha \lambda + \beta \mu) + \left( \frac{n C_j}{T} \right)^2 \lambda \mu (\alpha \beta - 1)} \right| H_0$$

$$\therefore \frac{1}{\lambda} = \left| \frac{H_0}{I} \right| = \frac{T^2 - n C_j (\alpha \lambda + \beta \mu) T + n^2 C_j^2 \lambda \mu (\alpha \beta - 1)}{C_j \left\{ T - n C_j \lambda \mu (2 + \alpha + \beta) \right\}} \quad (\text{Equ. 23})$$

As T increases  $\frac{1}{\lambda}$  approaches as asymptote a straight line with slope  $\frac{1}{C_j}$ . As T approaches a temperature given by the expression

$$\theta' = n C_j \lambda \mu (2 + \alpha + \beta), \quad (\text{Equ. 24})$$

$\frac{1}{\lambda}$  becomes infinite.

Therefore  $\frac{1}{\lambda}$  can be written in the form

$$\frac{1}{\lambda} = \frac{T}{C_j} + \frac{1}{\lambda_0} - \frac{\theta'}{T - \theta'} \quad (\text{Equ. 25})$$

$$\begin{aligned} \therefore \frac{1}{\lambda_0} &= \lim_{T \rightarrow \infty} \left( \frac{1}{\lambda} - \frac{T}{C_j} \right) = \lim_{T \rightarrow \infty} \frac{-n C_j (\alpha \lambda + \beta \mu) T + n^2 C_j^2 \lambda \mu (\alpha \beta - 1) + \theta' T}{C_j (T - \theta')} \\ &= n \lambda \mu (2 + \alpha + \beta) - n (\alpha \lambda + \beta \mu) = n (2 \lambda \mu + \alpha \lambda \mu + \beta \lambda \mu - \alpha \lambda - \beta \mu). \end{aligned}$$

Since  $\mu + \lambda = 1$ :

$$\frac{1}{\lambda_0} = n (2 \lambda \mu - \alpha \lambda^2 - \beta \mu^2) \quad (\text{Equ. 26})$$

$$\begin{aligned} \sigma &= \lim_{T \rightarrow \Theta'} \frac{\Theta' - T}{\chi} = -\frac{1}{C_j} \lim_{T \rightarrow \Theta'} \left[ T^2 - nC_j(\alpha\lambda + \beta\mu)T + n^2C_j^2\lambda\mu(\alpha\beta - 1) \right] \\ &= n^2C_j\lambda\mu \left[ -4\lambda\mu - 2\alpha\lambda\mu - 2\beta\lambda\mu + 2\alpha\lambda^2 + 2\beta\mu^2 + \alpha^2\lambda^2 + \beta^2\mu^2 + \right. \\ &\quad \left. + \alpha\beta\mu^2 + \alpha\beta\lambda^2 - \alpha\beta + 1 \right] \end{aligned}$$

Since  $\lambda + \mu = 1$ ,  $\lambda^2 + \mu^2 + 2\lambda\mu = 1$ .

Therefore:

$$\sigma = n^2C_j\lambda\mu \left[ \lambda(1+\alpha)^2 - \mu(1+\beta) \right]^2 \quad (\text{Equ. 27})$$

$\frac{1}{\chi}$  is plotted in Figure 2, with  $\Theta'$  and  $\frac{1}{\chi_0}$  indicated.

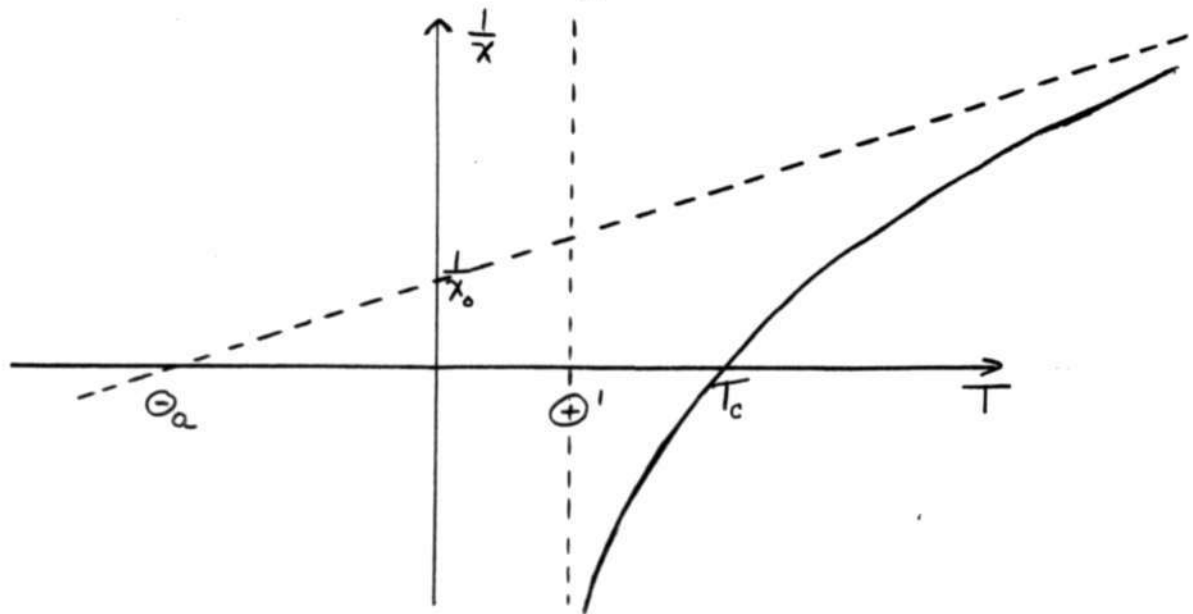


Figure 2: The reciprocal of ferrimagnetic susceptibility plotted vs. temperature

The parameter  $\Theta_a$  is defined as the intercept on the temperature axis of the asymptote  $y = \frac{T}{C_j} + \frac{1}{\chi_0}$ ; it is given by the equations

$$\Theta_a = -\frac{C_j}{\chi_0} = -nC_j(2\lambda\mu - \lambda^2\alpha - \mu^2\beta) \quad (\text{Equ. 28})$$

The parameters  $\theta'$ ,  $\frac{1}{\chi_0}$ ,  $\sigma$  and  $\theta_a$  can be obtained from susceptibility data as follows:

If the set of measurements at the highest temperature is denoted by the subscript M, then:

$$\frac{1}{\chi_M} = \frac{T_M}{C_j} + \frac{1}{\chi_0} - \frac{\sigma}{T_M - \theta'}$$

while for any other measurement

$$\frac{1}{\chi} = \frac{T}{C_j} + \frac{1}{\chi_0} - \frac{\sigma}{T - \theta'}$$

Subtracting:

$$\frac{1}{\chi_M} - \frac{1}{\chi} = \frac{T_M - T}{C_j} - \sigma \frac{T - T_M}{(T_M - \theta')(T - \theta')}$$

$$\therefore \frac{\frac{1}{\chi_M} - \frac{1}{\chi}}{T_M - T} = \frac{1}{C_j} + \frac{\sigma}{(T_M - \theta')(T - \theta')}$$

$$\left[ \frac{\frac{1}{\chi_M} - \frac{1}{\chi}}{T_M - T} - \frac{1}{C_j} \right]^{-1} = \frac{T_M - \theta'}{\sigma} (T - \theta')$$

$$\left[ \frac{\frac{1}{\chi_M} - \frac{1}{\chi}}{T_M - T} - \frac{1}{C_j} \right]^{-1} = \frac{(T_M - \theta')^2}{\sigma} - \frac{T_M - \theta'}{\sigma} (T_M - T)$$

Therefore when the left-hand side of this equation is plotted vs.  $T_M - T$  with experimental data substituted for  $\frac{1}{\chi_M}$ ,  $\frac{1}{\chi}$ ,  $T_M$ , and  $T$ , and if  $C_j$  is assumed to be known, a straight line would result with ordinate intercept  $\frac{(T_M - \theta')^2}{\sigma}$  and

with slope  $\sigma$ .  $\frac{1}{\lambda_0}$  can then be found by taking the average value over all observations of the function

$$\frac{1}{\lambda_0} = \frac{1}{\lambda} - \frac{T}{C_j} + \frac{\sigma}{T - \theta'}$$

When  $\frac{1}{\lambda_0}$ ,  $\sigma$  and  $\theta'$  are found, it is possible to compute the exchange integrals  $n$ ,  $\alpha$ , and  $\beta$  by solving Equations (27), (26) and (24).

These can be written as simultaneous linear equations in  $\alpha$ ,  $\beta$  and  $n$ :

$$\lambda \alpha - \mu \beta \mp \sqrt{\frac{\sigma}{C \lambda \mu}} \frac{1}{n} = \mu - \lambda$$

$$\lambda^2 \alpha + \mu^2 \beta + \frac{1}{\lambda_0} \frac{1}{n} = 2 \lambda \mu$$

$$\alpha + \beta - \frac{\theta'}{C \lambda \mu} \frac{1}{n} = -2$$

The solutions are:

$$\alpha = \frac{1}{n} \left( \frac{\mu \theta'}{\lambda C_j} - \frac{1}{\lambda_0} \mp 2 \mu \sqrt{\frac{\sigma}{C \lambda \mu}} \right) \quad (\text{Equ. 29})$$

$$\beta = \frac{1}{n} \left( \frac{\lambda \theta'}{\mu C_j} - \frac{1}{\lambda_0} \mp 2 \lambda \sqrt{\frac{\sigma}{C \lambda \mu}} \right) \quad (\text{Equ. 30})$$

$$n = \frac{\theta'}{C_j} + \frac{1}{\lambda_0} \mp (\mu - \lambda) \sqrt{\frac{\sigma}{C \lambda \mu}} \quad (\text{Equ. 31})$$

Thus one set of  $\theta'$ ,  $\sigma$  and  $\frac{1}{\lambda_0}$  may correspond to two different sets of  $\alpha$ ,  $\beta$ , and  $n$ . With the values of  $\alpha$ ,  $\beta$ , and  $n$  obtained from data above the Curie temperature, the spontaneous magnetization below the Curie temperature can be calculated as a function of the temperature. By comparison with experimental curves for the magnetization a choice between the two sets of exchange integrals can usually be made quite easily.

D. The Curie Temperature; Spontaneous magnetization at the Curie Temperature

The four equations of state (Equations 12, 13, 14, and 15) can be solved at high temperature by means of the linear approximation expressed by Equations 20 and 21. In the absence of an external field, these become:

$$\left(1 - \frac{nC_j}{T} \alpha \lambda\right) I_a - \frac{nC_j}{T} \mu I_b = 0 \quad (\text{Equ. 32})$$

$$- \frac{nC_j}{T} \lambda I_a + \left(1 - \frac{nC_j}{T} \beta \mu\right) I_b = 0 \quad (\text{Equ. 33})$$

The solutions  $I_a = I_b = 0$  correspond to paramagnetism: in the absence of an external field the magnetization is zero. However, non-vanishing solutions can be obtained when the determinant of the coefficients of  $I_a$  and  $I_b$  vanishes:

$$\left(1 - \frac{nC_j}{T} \alpha \lambda\right) \left(1 - \frac{nC_j}{T} \beta \mu\right) = \frac{n^2 C_j^2}{T^2} \lambda \mu \quad (\text{Equ. 34})$$

This occurs at two temperatures which satisfy the quadratic Equation 34, which can be rewritten:

$$T^2 - nC_j T (\alpha \lambda + \beta \mu) - n^2 C_j^2 \lambda \mu (1 - \alpha \beta) = 0$$

The two solutions are given by:

$$T_c = \frac{nC_j}{2} \left[ (\alpha \lambda + \beta \mu) + \sqrt{(\alpha \lambda - \beta \mu)^2 + 4 \lambda \mu} \right] \quad (\text{Equ. 35a})$$

$$T_c' = \frac{nC_j}{2} \left[ (\alpha \lambda + \beta \mu) - \sqrt{(\alpha \lambda - \beta \mu)^2 + 4 \lambda \mu} \right] \quad (\text{Equ. 35b})$$

$$T_c + T_c' = nC_j (\alpha \lambda + \beta \mu) \quad (\text{Equ. 36})$$

$$T_c T_c' = n^2 C_j^2 \lambda \mu (\alpha \beta - 1) \quad (\text{Equ. 37})$$

From the sign of the expressions for  $T_c + T_c'$  and  $T_c T_c'$  the following conclusions can be drawn about the sign and relative magnitudes of  $T_c$  and  $T_c'$ :

If:	$T_c + T_c' < 0$	$T_c + T_c' > 0$
$T_c T_c' < 0$	One root positive,	the other negative
$T_c T_c' > 0$	$T_c$ and $T_c'$ both negative	$T_c$ and $T_c'$ both positive

From Equation 37 it is thus seen that when  $\alpha\beta < 1$  (i.e.  $T_c T_c' < 0$ ), there is at least one positive root, while when  $\alpha\beta > 1$  (i.e.  $T_c T_c' > 0$ ) there can only be a positive root if  $\alpha\lambda + \beta\mu > 0$  (i.e.  $T_c + T_c' > 0$ ). In Figure 3 a map is plotted with ordinate  $\beta$  and abscissa  $\alpha$ , so that each point in this map represents a pair of values of  $\alpha$  and  $\beta$ .

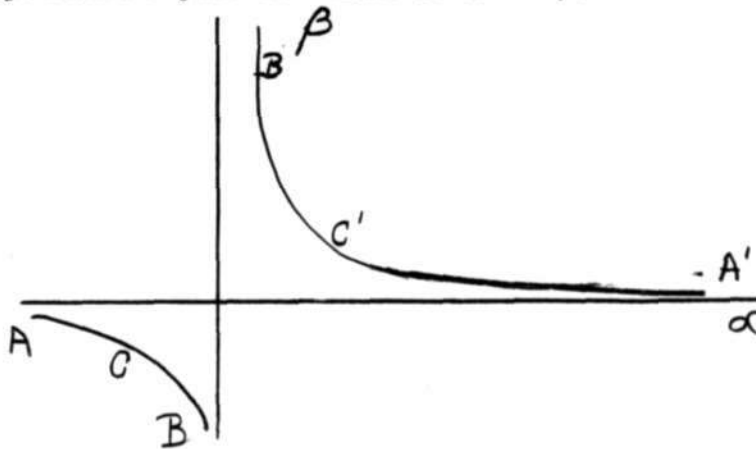


Figure 3: Map of  $\alpha$ - $\beta$  values giving paramagnetism or ferrimagnetism

The curves  $ACB$  and  $A' C' B'$  are the locus of the points  $\alpha\beta = 1$ . Between these curves  $\alpha\beta < 1$ , outside them  $\alpha\beta > 1$ . In the region between the curves there exists one positive root of Equation 34. Below and to the left of  $ACB$  no positive root exists, for here  $\alpha < 0$ ,  $\beta < 0$ , hence  $(\alpha\lambda + \beta\mu) < 0$ . Above and to the right of  $A' C' B'$  there are two positive roots of Equation 34. When the values of  $\alpha$  and  $\beta$  are such that in Figure 3 the representative point lies to the right and above the curve  $ACB$ , a temperature exists at which spontaneous magnetization is possible. When the representative point lies below and to the left of  $ACB$  spontaneous magnetization is impossible at all

temperatures, so that the substance is paramagnetic.

To find the spontaneous magnetization at the critical temperatures given by Equations 35a and 35b, substitute these temperatures with Equations 32 or 33, and solve for  $\frac{I_a}{I_b}$ . (Since Equations 32 and 33 are homogeneous, they do not give two independent values of  $I_a$  and  $I_b$ , but only their ratio.)

Equation 32 can be rewritten for the temperature  $T = T_c$ :

$$I_a (T_c - nC_j \alpha \lambda) = nC_j \mu I_b$$

Equation 35a gives:

$$T_c - nC_j \alpha \lambda = \frac{nC_j}{2} \left[ -(\alpha \lambda - \beta \mu) + \sqrt{(\alpha \lambda - \beta \mu)^2 + 4 \lambda \mu} \right]$$

Dividing the last two equations gives:

$$\frac{I_b}{I_a} = \frac{-(\alpha \lambda - \beta \mu) + \sqrt{(\alpha \lambda - \beta \mu)^2 + 4 \lambda \mu}}{2\mu} \quad (\text{Equ. 38a})$$

Therefore for the solution  $T = T_c$ ,  $I_a$  and  $I_b$  have the same sign, so that in this case  $\vec{I}_a$  and  $\vec{I}_b$  are antiparallel in accordance with the definitions given with Section B.

If Equation 35b had been substituted into Equation 32, the result would have been:

$$\frac{I_b}{I_a} = \frac{-(\alpha \lambda - \beta \mu) - \sqrt{(\alpha \lambda - \beta \mu)^2 + 4 \lambda \mu}}{2\mu}$$

In this case  $\vec{I}_a$  would have been parallel to  $\vec{I}_b$ . However, since  $T_c > T_c'$ , the antiparallel arrangement is more stable, for the energy corresponding to antiparallel arrangement is of the order of  $kT_c$ , which is larger than  $kT_c'$ , the energy corresponding to parallel arrangement.

It was shown in Section B that  $\vec{I}$  is parallel to  $\vec{I}_a$  if  $\lambda I_a > \mu I_b$ , and parallel to  $\vec{I}_b$  if  $\mu I_b > \lambda I_a$ .

$$\begin{aligned} \text{The expression } \lambda I_a - \mu I_b > 0 & \text{ if } \frac{I_b}{I_a} < \frac{\lambda}{\mu} \\ & = 0 \text{ if } \frac{I_b}{I_a} = \frac{\lambda}{\mu} \\ & < 0 \text{ if } \frac{I_b}{I_a} > \frac{\lambda}{\mu} \end{aligned}$$

$\frac{I_b}{I_a}$  is given by Equation 38a. Therefore

$$\begin{aligned} \lambda I_a - \mu I_b \gtrless 0 & \text{ if } \lambda \gtrless \frac{-(\alpha\lambda - \beta\mu) + \sqrt{(\alpha\lambda - \beta\mu)^2 + 4\lambda\mu}}{2} \\ \text{i.e. if } 2\lambda + \alpha\lambda - \beta\mu & \gtrless \sqrt{(\alpha\lambda - \beta\mu)^2 + 4\lambda\mu} \\ \text{i.e. if } \lambda(1+\alpha) & \gtrless \mu(1+\beta) \end{aligned}$$

In Figure 4 the  $\alpha\beta$  map is drawn again. The line SD represents the Equation  $\lambda(1+\alpha) = \mu(1+\beta)$ . Above and to the left of this line  $\lambda(1+\alpha) < \mu(1+\beta)$ , hence  $\vec{I}$  is parallel to  $\vec{I}_b$  for this region. In the region below and to the right of the line  $\vec{I}$  is parallel to  $\vec{I}_a$ .

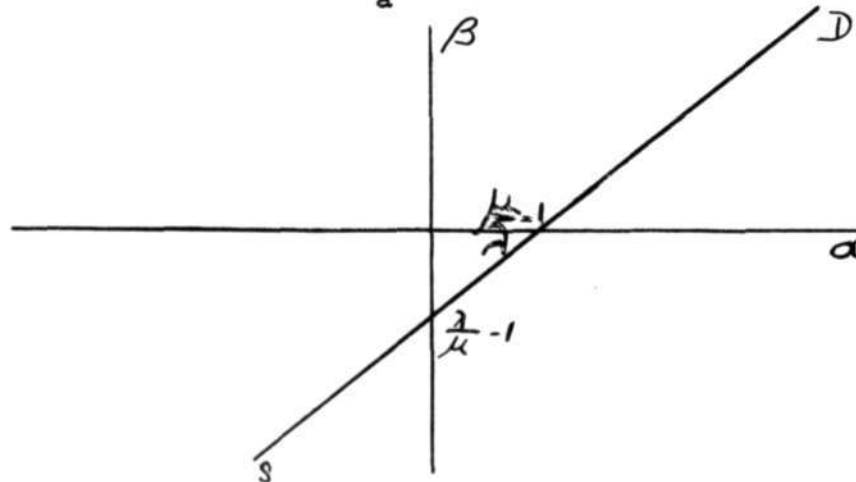


Figure 4: Map of  $\alpha\beta$  with curve separating the regions where the spontaneous magnetization at the Curie point is parallel to  $I_b$  from that where it is parallel to  $I_a$ .

E. Magnetization and its Temperature Coefficient at Absolute Zero of Temperature

At absolute zero the equations of state are easily solved. These equations are written below for  $H_0 = 0$ .

$$h_a = n(\alpha \lambda I_a + \mu I_b) \quad (\text{Equ. 12})$$

$$h_b = n(\beta \mu I_b + \lambda I_a) \quad (\text{Equ. 13})$$

$$I_a = M B_j \left( \frac{M h_a}{RT} \right) \quad (\text{Equ. 14'})$$

$$I_b = M B_j \left( \frac{M h_b}{RT} \right) \quad (\text{Equ. 15'})$$

When  $T = 0$  the argument of  $B_j$  is infinite if  $h_a \neq 0$  or  $h_b \neq 0$ ; when  $h_a = 0$  or  $h_b = 0$ , the argument is indeterminate.  $B_j(\infty) = 1$ , while when  $0 \leq z < \infty$ ,  $0 \leq B_j(z) < 1$ .

Accordingly, when  $h_a \neq 0$ ,  $I_a = M$  at  $T = 0$   
and when  $h_b \neq 0$ ,  $I_b = M$

The only way for  $I_a$  and  $I_b$  to differ from  $M$  is for  $h_a$  and  $h_b$  respectively to be zero. The following cases are therefore considered:

Case I:  $0 \leq I_a < M$ ;  $0 \leq I_b < M$

Case II:  $I_a = I_b = M$

Case III:  $I_a = M$ ;  $0 < I_b < M$

Case IV:  $0 \leq I_b < M$ ;  $I_a = M$ .

Case I. In order for  $I_a$  and  $I_b$  both to be zero, both  $h_a$  and  $h_b$  must vanish. Equations (12) and (13) then give:

$$\alpha \lambda I_a + \mu I_b = 0$$

$$\lambda I_a + \beta \mu I_b = 0$$

Then  $I_a = I_b = 0$  unless  $\alpha\beta = 1$

When  $\alpha\beta = 1$ ,  $T_c T_c' = 0$  according to Equation 37, so that the Curie point is just at absolute zero, and Section D would be applicable. Therefore unless the substance happens to have a Curie point at absolute zero, Case I is limited to  $I_a = I_b = 0$ , which indicates paramagnetism.

Case II. When  $I_a = I_b = M$ , Equations (12) and (13) give:

$$h_a = nM(\alpha\lambda + \mu)$$

$$h_b = nM(\lambda + \beta\mu)$$

In order for  $I_a$  and  $I_b$  to be positive, a basic assumption for ferri-magnetism,  $h_a$  and  $h_b$  must be positive, hence:

$$\alpha\lambda + \mu > 0, \therefore \alpha > -\frac{\mu}{\lambda}$$

$$\lambda + \beta\mu > 0, \therefore \beta > -\frac{\lambda}{\mu}$$

Therefore Case II is limited to the region to the right of and above the lines  $\alpha = -\frac{\mu}{\lambda}$  and  $\beta = -\frac{\lambda}{\mu}$  drawn in the  $\alpha\beta$  map in Figure 5.

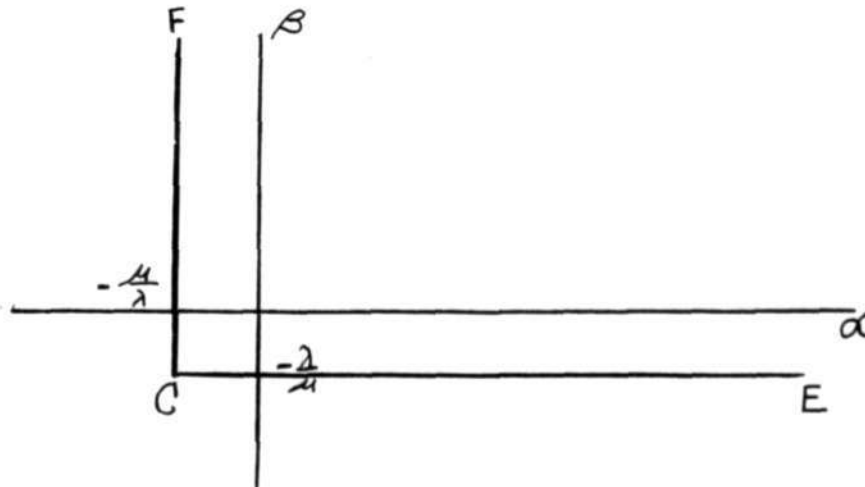


Figure 5: Map of  $\alpha$  vs.  $\beta$  delineating the region where Case II holds

Case III. In order for  $I_b$  to be less than  $M$ ,  $h_b = 0$ .

Substituting  $I_a = M$ ,  $h_b = 0$  into Equation 13 gives:

$$I_b = -\frac{\lambda}{\beta\mu} M \quad (\text{Equ. 39})$$

Since  $0 < I_b < M$ ,  $-\frac{\lambda}{\beta\mu} < 1$ ; hence Case III is limited to the region below the line CE in Figure 5,

Case IV. In order for  $I_a$  to be less than  $M$ ,  $h_a = 0$

Substituting  $I_b = M$ ,  $h_a = 0$  into Equation 12 gives:

$$I_a = -\frac{\mu}{\alpha\lambda} M \quad (\text{Equ. 40})$$

Since  $0 < I_a < M$ ,  $-\frac{\mu}{\alpha\lambda} < 1$ , so that Case IV is limited to the region to the left of the line CF in Figure 5.

Figure 6 is a superposition of 3 and 5.

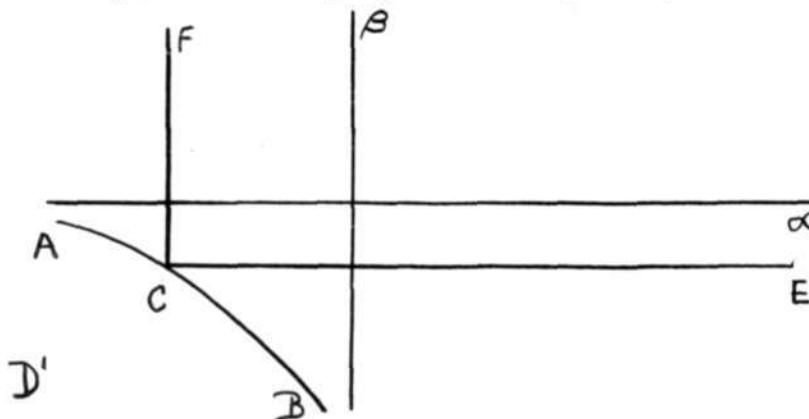


Figure 6: Cases I, II, III, and IV delineated on the  $\alpha\beta$  map

Case I holds in the region ACBD'

Case II holds in the region FCE

Case III holds in the region BCE

Case IV holds in the region ACF

The saturation magnetization can be found from Equation 9a and is listed in Table II, together with the molecular fields:

Table II

Case	$h_a$	$h_b$	$\lambda I_a$	$\mu I_b$	I	Direction of $\vec{I}$
I	0	0	0	0	0	
II	$nM(\alpha\lambda+\mu)$	$nM(\beta\mu+\lambda)$	$\lambda M$	$\mu M$	$(\mu-\lambda)M^*$	parallel to $I_b^*$
III	$n\lambda M(\alpha-\frac{1}{\beta})$	0	$\lambda M$	$-\frac{\lambda}{\beta} M$	$(1+\frac{1}{\beta})M$	parallel to either, see below
IV	0	$n\mu M(\beta-\frac{1}{\alpha})$	$-\frac{\mu}{\alpha} M$	$\mu M$	$-(1+\frac{1}{\alpha})\mu M$	parallel to $I_b$

According to Equation 9a  $\vec{I}$  is parallel to  $\vec{I}_a$  only if  $\mu I_b > \lambda I_a$ . Since case IV is limited to the region  $\alpha < -\frac{\mu}{\lambda} <^* -1$ ,  $-\frac{1}{\alpha} < 1$ , so that  $-\frac{\mu}{\alpha} M < \mu M$ , i.e.  $\lambda I_a < \mu I_b$ . Thus Case IV corresponds to  $\vec{I}$  parallel to  $\vec{I}_b$ . In Case III, however,  $\beta < -\frac{\lambda}{\mu}$ , which may or may not be less than unity. If  $\beta > -1$ ,  $-\frac{1}{\beta} > 1$ ;  $\therefore \mu I_b > \lambda I_a$ , and  $\vec{I}$  is parallel to  $\vec{I}_b$ . If  $\beta < -1$ ,  $-\frac{1}{\beta} < 1$ ;  $\therefore \mu I_b < \lambda I_a$ , and  $\vec{I}$  is parallel to  $\vec{I}_a$ .

In Figure 7 is drawn the line  $\beta = -1$  as well as the line SC of Figure 4.

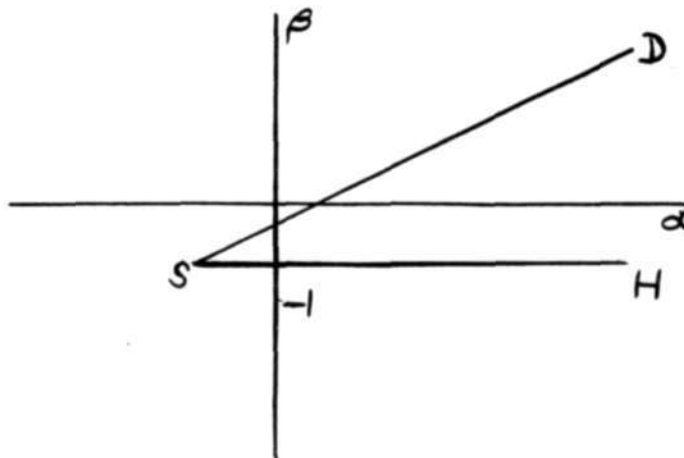


Figure 7: Lines delineating saturation magnetization directions at absolute zero and at the Curie temperature

It was seen that at the Curie temperature the region above SD corresponds to  $\vec{I}$  parallel to  $\vec{I}_b$ , and the region below SD to  $\vec{I}$  parallel to  $\vec{I}_a$ . At absolute zero the region above SH corresponds to  $\vec{I}$  parallel to  $\vec{I}_b$ ,

\* because  $\mu \geq \lambda$ .

the one below SH to  $\vec{I}$  parallel to  $\vec{I}_a$ . Thus the region above SD corresponds to  $\vec{I}$  parallel to  $\vec{I}_b$ , the region below SH to  $\vec{I}$  parallel to  $\vec{I}_a$ , while in the region DSH the magnetization is parallel to  $\vec{I}_a$  at the Curie temperature, and parallel to  $\vec{I}_b$  at the absolute zero. This indicates that as the temperature is decreased from Curie temperature to absolute zero, the magnetization passes through zero and reverses its direction. The temperature at which this reversal occurs is called the "Compensation temperature"; at this temperature  $\lambda I_a = \mu I_b$ .

The temperature coefficient of magnetization at absolute zero can be found for each of the four cases discussed above.

Case I. When  $I_a = I_b = 0$  at  $T = 0$ , the magnetization is certainly zero above the absolute zero temperature, for this case corresponds to a paramagnetic system.

When  $T > 0$  and  $h_a = 0$  in Equation 14',  $I_a = 0$ , but then according to Equation 12  $I_b = 0$ , which in turn leads to  $h_b = 0$  in Equation 13, and consequently to  $I_b = 0$  in Equation 15'. Thus  $I_a = I_b = 0$  is a solution of the equations of state even when  $T > 0$ .

Case II. When  $I_a = I_b = M$  at  $T = 0$ , the magnetization just above absolute zero can be expanded in terms of the magnetization at  $T = 0$ , for when  $z$  is large,  $B_j(z) \doteq 1 - \frac{1}{j} \exp\left[-\frac{z}{j}\right]$ .

$$\therefore I_a \doteq M \left[ 1 - \frac{1}{j} \exp \left\{ -\frac{n}{j} \left( \frac{\alpha \lambda I_a + \mu I_b}{RT} \right) \right\} \right]$$

$$I_b \doteq M \left[ 1 - \frac{1}{j} \exp \left\{ -\frac{n}{j} \left( \frac{\beta \mu I_b + \lambda I_a}{RT} \right) \right\} \right]$$

It was shown (see Table II) that for Case II  $\vec{I}$  is parallel to  $\vec{I}_b$ .

Then 
$$I = \mu I_b - \lambda I_a = (\mu - \lambda) + \frac{\lambda}{j} M e^{-\frac{n}{j} \frac{\alpha\lambda + \mu}{RT}} - \frac{\mu}{j} M e^{-\frac{n}{j} \frac{\beta\mu + \lambda}{RT}}$$

$$\therefore \frac{\partial I}{\partial T} = \frac{n\lambda}{j^2} \frac{(\alpha\lambda + \mu)}{RT^2} e^{-\frac{n}{j} \frac{\alpha\lambda + \mu}{RT}} - \frac{n\mu}{j^2} \frac{(\beta\mu + \lambda)}{RT^2} e^{-\frac{n}{j} \frac{(\beta\mu + \lambda)}{RT}} M$$
  
 If  $(\alpha\lambda + \mu) > (\beta\mu + \lambda)^*$

$$\frac{\partial I}{\partial T} = \frac{n}{j^2 RT^2} e^{-\frac{n}{j} \frac{(\beta\mu + \lambda)}{RT}} M \left[ \lambda(\alpha\lambda + \mu) e^{-\frac{n}{j} \frac{(\alpha-1)\lambda + (\beta-1)\mu}{RT}} - \mu(\beta\mu + \lambda) \right]$$

Then for very small T the first term in the brackets becomes negligible, while the second term is independent of temperature. Therefore for small T  $\frac{\partial I}{\partial T} < 0$ . As  $T \rightarrow 0$  the coefficient of the bracketed expression vanishes, so that  $(\frac{\partial I}{\partial T})_{T=0} = 0$

If  $(\beta\mu + \lambda) > (\alpha\lambda + \mu)$ ,

$$\frac{\partial I}{\partial T} = \frac{n}{j^2 RT^2} e^{-\frac{n}{j} \frac{(\alpha\lambda + \mu)}{RT}} M \left[ \lambda(\alpha\lambda + \mu) - \mu(\beta\mu + \lambda) e^{-\frac{n}{j} \frac{(\beta-1)\mu + (\alpha-1)\lambda}{RT}} \right]$$

In this case for very low T the second term vanishes, so that now  $\frac{\partial I}{\partial T} \geq 0$  for low T, and  $\lim_{T \rightarrow 0} \frac{\partial I}{\partial T} = 0$ .

In Figure 8 is drawn the line CK with Equation  $\beta\mu + \lambda = \alpha\lambda + \mu$  separating regions in the  $\alpha\beta$  map with positive temperature coefficient of magnetization from those with a negative temperature coefficient at low temperature. To the left and above the line CK  $\beta\mu + \lambda > \alpha\lambda + \mu$ , so that in this region  $\frac{\partial I}{\partial T} \geq 0$ , while below and to the right of this line  $\frac{\partial I}{\partial T} \leq 0$ .

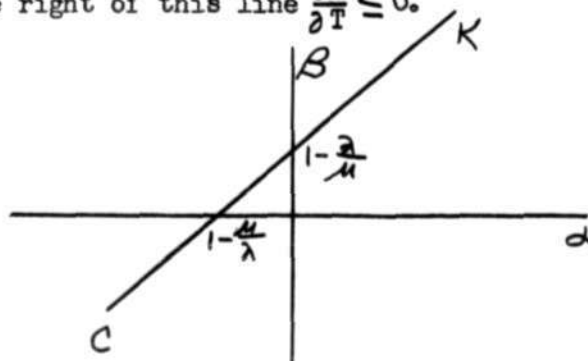


Figure 8: Line separating regions with positive and negative temperature coefficients of magnetization at low temperatures.

\* For Case II  $\alpha > -\frac{\mu}{\lambda}$ ,  $\therefore \alpha\lambda + \mu > 0$ , and  $\beta > -\frac{\lambda}{\mu}$ ,  $\therefore \beta\mu + \lambda > 0$ .

Case III. When  $T = 0$ ,  $I_a = M$ ,  $0 < I_b < M$ ,  $h_a > 0$ ,  $h_b = 0$ . At very low temperatures  $h_b$ , while different from zero, is still small compared to  $h_a$ . When  $T$  is very small,  $Mh_a \gg RT$ , so that from Equation 14 it appears that  $I_a = M$ .

$$\text{Therefore } \frac{dI_a}{dT} = 0.$$

For Case III, as shown in Table I and below it.

$$I = \mu I_b - \lambda I_a \text{ for } \beta > -1$$

$$I = \lambda I_a - \mu I_b \text{ for } \beta < -1$$

$$\therefore \frac{dI}{dT} = \mu \frac{dI_b}{dT} \text{ for } \beta > -1$$

$$\frac{dI}{dT} = -\mu \frac{dI_b}{dT} \text{ for } \beta < -1$$

Differentiating Equation 13 with respect to  $T$  gives:

$$\frac{dh_b}{dT} = n\beta\mu \frac{dI_b}{dT}$$

$$\therefore \frac{dI}{dT} = \frac{1}{n\beta} \frac{dh_b}{dT} \text{ for } \beta > -1$$

$$\frac{dI}{dT} = -\frac{1}{n\beta} \frac{dh_b}{dT} \text{ for } \beta < -1$$

However, for Case III  $\beta < -\frac{\lambda}{\mu}$ , so that

$$\frac{dI}{dT} < 0 \text{ for } \beta > -1$$

$$\frac{dI}{dT} > 0 \text{ for } \beta < -1$$

The above analysis is shown graphically in Figure 9 by plotting the two equations of state Equation 13 and Equation 15 in one  $I_b$  vs.  $h_b$  graph. The solution of these equations is then given by the intersection of these two curves. Equation 15 is drawn for various values of  $T$ ; Equation 13 is not explicitly dependent on  $T$ .

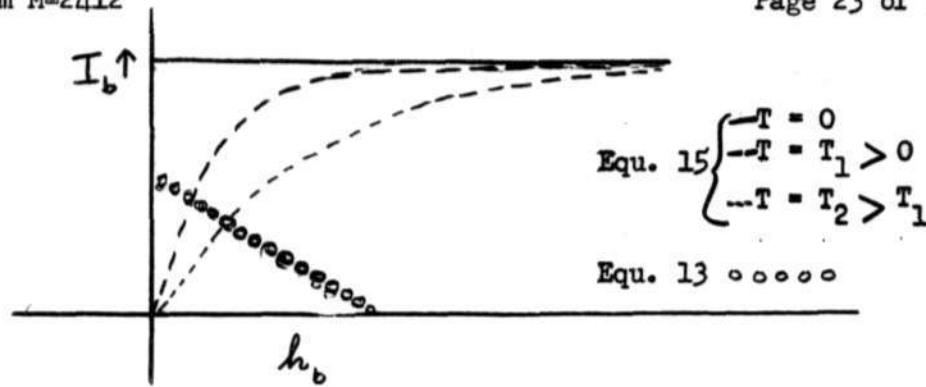


Figure 9: Equation 13 and 15 plotted for various values of T.

It is easily seen that as  $h_b$  increases from zero and the curves change from the solid one, the value of  $I_b$  decreases appreciably.

In Figure 10 are drawn the Equations 12 and 14; as  $I_a = M$ , Equation 12 is represented by a practically horizontal line; any change in  $I_a$  due to a change in  $h_a$  is offset by the change in  $I_b$  just discussed. Therefore the intersection always corresponds to partially the same value of  $I_a$ .

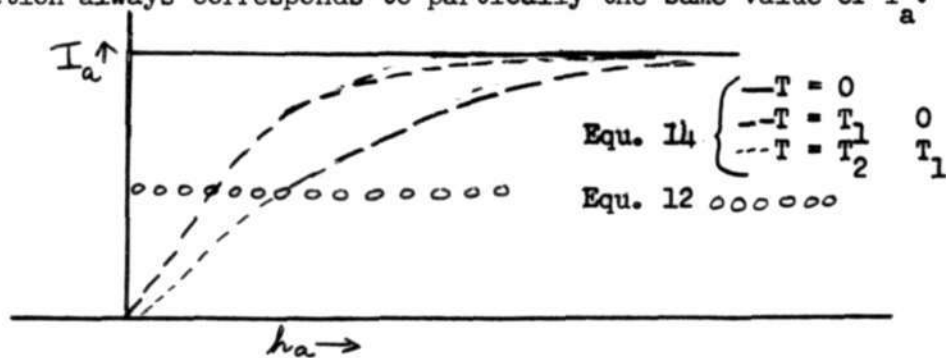


Figure 10: Equations 12 and 14 plotted for various values of T

Physically this case may be summarized as follows: When  $\beta > -1$  the B sites are dominant because of their purity ( $\mu > \lambda$ ). Therefore the total magnetization is due to the magnetization of the B sites which is partially canceled out by that of the A sites. As the temperature increases, the magnetization of the A sites remains about constant, while that due to the B sites decreases, so that the net effect is a decrease in magnetization.

When  $\beta < -1$ , the B-B interaction can no longer compete with the stronger A-A parallel interaction, so that the A sites become dominant in spite of their numerical minority. The magnetization is now due to that of the A sites, which is partially canceled out by that of the B sites. Since an increase in temperature decreases this cancellation, the net magnetization increases with temperature.

Case IV. The reasoning in this case is analogous to that in Case III; now  $\frac{dI_b}{dT} = 0$ , while  $\frac{dI_a}{dT} < 0$ . In this case, however,

$$I = \mu I_b - \lambda I_a \text{ for all values of } \alpha < -\frac{\mu}{\lambda}.$$

$$\therefore \frac{dI}{dT} = -\lambda \frac{dI_a}{dT} > 0.$$

Summary of Section E:

Figure 11 consists of a superposition of Figures 6, 7, 8.

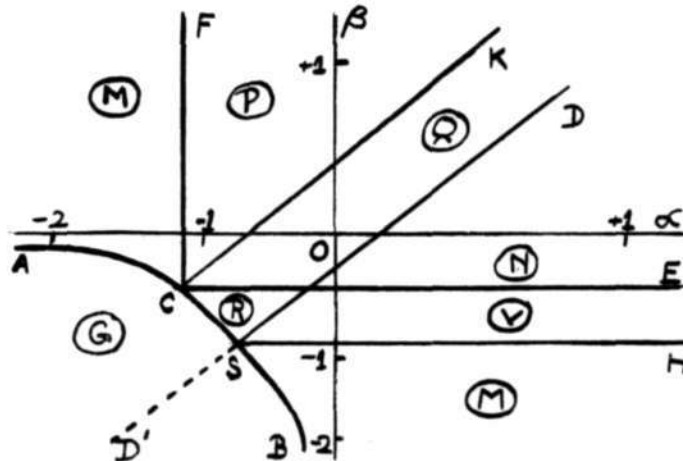


Figure 11: Diagram giving, as a function of  $\alpha$  and  $\beta$ , the different types of magnetization curves for negative interaction, between sites ( $\zeta = -1$ ). The figure is drawn for  $\frac{\lambda}{\mu} = \frac{2}{3}$

In region ACF, the magnetization is parallel to  $\vec{I}_b$  at all temperatures, and the temperature coefficient is positive at  $T = 0$ , so that curve 12M results for the magnetization vs. temperature.

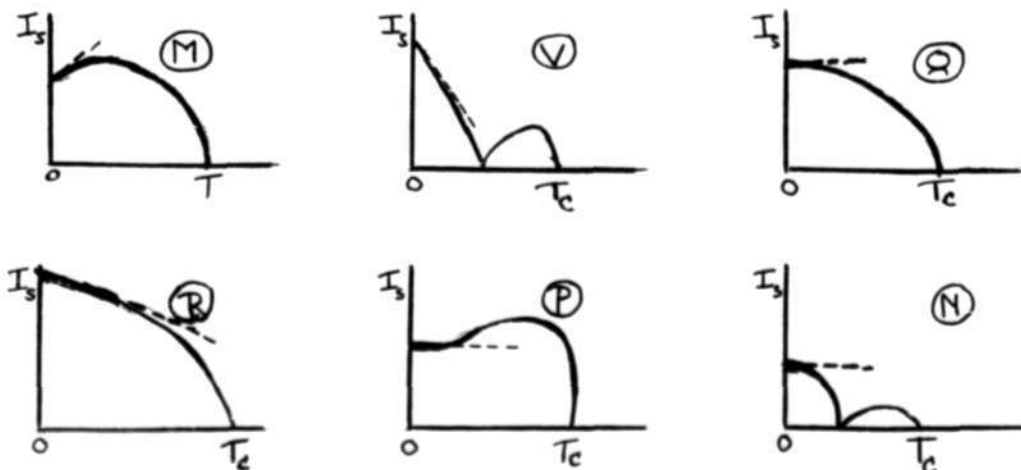


Figure 12: Principal Types of Magnetizations

In region P the temperature coefficient is zero at absolute zero, and positive at low positive temperatures. The magnetization is everywhere parallel to  $\vec{I}_b$ , so that curve 12P results. In region Q the temperature coefficient is zero at absolute zero, negative at low positive temperatures. The magnetization is always parallel, so that Figure 12 Q results.

In region N the magnetization is parallel to  $\vec{I}_b$  at zero temperature, and to  $\vec{I}_a$  at the Curie temperature. The temperature coefficient is zero at  $T = 0$  and decreases with increasing temperature, so that Figure 12 N results for the absolute magnitude of the magnetization as a function of temperature.

In region R the temperature coefficient is negative at absolute zero and above; the magnetization is everywhere parallel to  $\vec{I}_b$ , so that Figure 12 R results.

In region V the temperature coefficient is negative, the magnetization is parallel to  $\vec{I}_b$  at  $T = 0$  and to  $\vec{I}_a$  at the Curie temperature, so that Figure 12 V results.

In region BSH the magnetization is parallel to  $\vec{I}_a$  and the temperature coefficient is positive at all low temperatures, so that curve 12 M results. Regions ACF and BSH therefore give rise to the same type of magnetization curve.

#### F. Antiferromagnetism: a special case of ferrimagnetism

A particular case of ferrimagnetism that is rather common and not easily detected is called antiferromagnetism. It corresponds to the situation when  $\lambda = \mu$  and  $\alpha = \beta$ . Since mathematically some of the expressions derived for ferrimagnetism generally become indeterminate, and since some of the physical properties of antiferromagnetism are so remarkable and were not explained until Néel's molecular field theory for ferrimagnetism was formulated, the behavior at relatively high temperatures, at the Curie point (if there is one) and near absolute zero will be discussed here.

The equations of state can be written for antiferromagnetic materials:

$$h_a = \frac{n}{2} (\alpha I_a + I_b) \quad (\text{Equ. 41})$$

$$h_b = \frac{n}{2} (I_a + \alpha I_b) \quad (\text{Equ. 42})$$

$$\vec{I}_a = MB_j \left[ \frac{M}{RT} (\vec{H}_o + \vec{h}_a) \right] \quad (\text{Equ. 43})$$

$$\vec{I}_b = MB_j \left[ \frac{M}{RT} (\vec{H}_o + \vec{h}_b) \right] \quad (\text{Equ. 44})$$

It is easily seen that  $I_a = I_b$  satisfies these equations, in which case also  $h_a = h_b$ . Therefore, since  $\lambda = \mu$ ,  $I = 0$ , so that in the absence of an external field the magnetization of antiferromagnetic materials is zero everywhere just as is the case in paramagnetic materials. Yet it will be shown below that the response to an external field, as expressed by the susceptibility, is quite different from that of paramagnetic materials.

The susceptibility was given by Equation 25:

$$\frac{1}{\chi} = \frac{T}{C_j} + \frac{1}{\chi_o} - \frac{\sigma}{T - \theta'} \quad (\text{Equ. 25})$$

In the case of antiferromagnetism the parameters can be written:

$$\theta' = \frac{n}{2} C_j (1+\alpha) \quad (\text{Equ. 45})$$

$$\frac{1}{\chi_o} = \frac{n}{2} (1-\alpha) \quad (\text{Equ. 46})$$

$$\sigma = 0 \quad (\text{Equ. 47})$$

$$\theta_a = -\frac{n}{2} C_j (1-\alpha) \quad (\text{Equ. 48})$$

Thus  $\frac{1}{\chi}$  is linearly proportional to  $T$  except where  $T = \theta'$ . When  $T = \theta'$  the fraction  $\frac{\sigma}{T - \theta'}$  is indeterminate.

The Curie temperature, as given in Equation 35a now becomes:

$$T_c = \frac{nC_j}{2} (1+\alpha) \quad (\text{Equ. 49})$$

$$\therefore T_c = \theta'.$$

The susceptibility is plotted as a function of temperature in Figure 13.

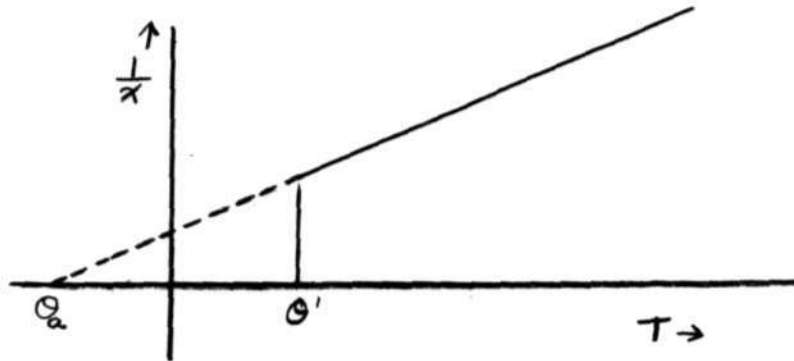


Figure 13:  $\frac{1}{\chi}$  vs.  $T$  for antiferromagnetic materials

Below the Curie point the arrangement of the electron spins is quite as orderly for antiferromagnetic as for all ferrimagnetic and ferromagnetic materials, but because of the exact cancellation of the magnetizations this does not give rise to spontaneous magnetization. Other properties besides the susceptibility, such as specific heat, show a marked discontinuity at the Curie temperature.

When  $\vec{H}_0$  is imposed parallel to  $\vec{h}_a$ , it is automatically antiparallel to  $\vec{h}_b$ . Since Equations 43 and 44 are not linear, the effect on  $\vec{I}_a$  of a given increase in the total magnetic field on the A sites is not exactly matched by the effect on  $\vec{I}_b$  due to an equal decrease in the magnetic field on the B sites. This is demonstrated in Figure 14. When  $\vec{H}_0$  is applied parallel to  $\vec{h}_a$ , the magnitude of the total field on the A sites is increased from  $h$  to  $h + H_0$ , resulting in an increase in  $I_a$  by an amount  $\Delta I_a$ . But  $\vec{H}_0$  is antiparallel to  $\vec{h}_b$ , so that the magnitude of the total field on the B sites is decreased from  $h$  to  $h - H_0$ , resulting in a decrease in  $I_b$  by an amount  $\Delta I_b$ . Since the magnetization curve drawn in Figure 14 levels off toward higher fields, the increase in  $I_a$ ,  $\Delta I_a$ , is less than the decrease in  $I_b$ ,  $\Delta I_b$ . Therefore  $\vec{I}_a$  and  $\vec{I}_b$  no longer cancel each other precisely, so that a net magnetization is brought about by  $\vec{H}_0$ . Therefore the susceptibility is finite below the Curie temperature. It should be recalled, however, the magnetization curve changes with temperature as shown in Figures 9 and 10, so that at very low temperatures the effect of a change in total field on the magnetization of the A and B sites becomes negligible. The susceptibility therefore vanishes as the temperature goes to zero.

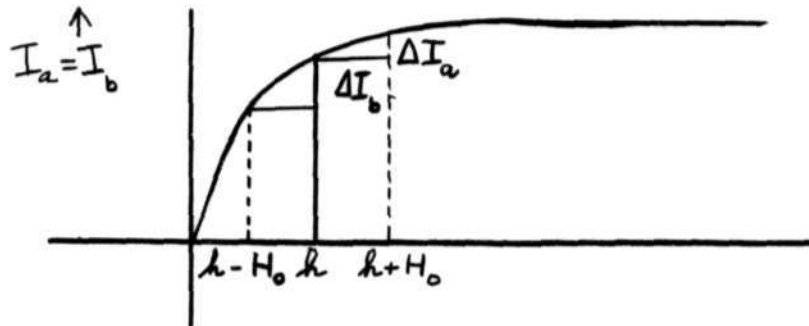


Figure 14: The effect of an external field on the magnetization of the A and B sites.

Since antiferromagnetic materials have no spontaneous magnetization, susceptibility measurements are not usually made with  $H_0$  exactly parallel or antiparallel to  $h_a$  and  $h_b$ . The perpendicular component of the field has merely the effect of deflecting the electron spins from their preferred direction as shown in Figure 15. This deflection is independent of the temperature, and hence gives rise to a constant susceptibility.

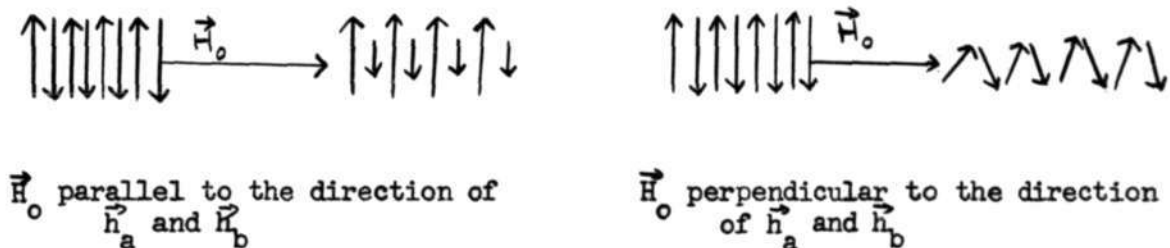


Figure 15: Effect of an external magnetic field on the magnetization of antiferromagnetic materials

In Figure 16 is shown the susceptibility as a function of temperature below the Curie point.

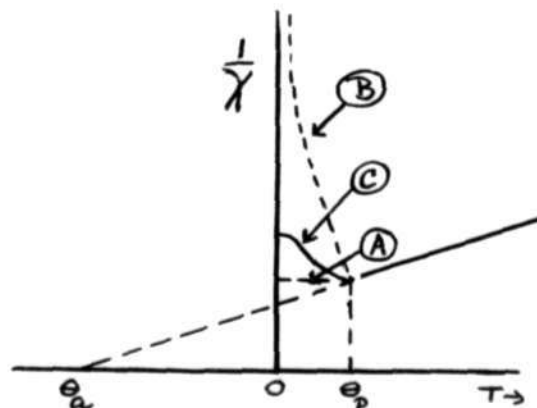


Figure 16: Thermal variation of inverse susceptibility for antiferromagnetics

In A, the spin direction is perpendicular to applied field  
 In B, it is parallel to applied field  
 In C, it is at some angle in between

In conclusion it might be interesting to draw Figure 11 for the special case  $\lambda = \mu$ . This is done in Figure 17.

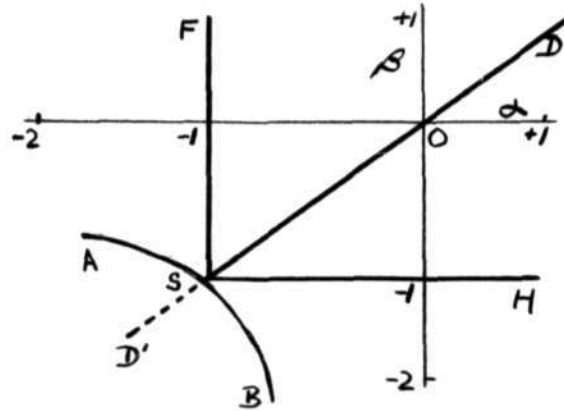


Figure 17: Diagram for determination, as a function of  $\alpha$  and  $\beta$  of the magnetization curves for  $\lambda = \mu$  and  $\xi = -1$

Antiferromagnetic materials are all represented by the line  $SD(\alpha=\beta)$ . At absolute zero the magnetization of all materials with  $\lambda = \mu$  is zero, but at higher temperatures only antiferromagnetic materials have zero magnetization; for all other materials with  $\lambda = \mu$  the magnetization curves drawn in Figure 12 now look as drawn in Figure 18.

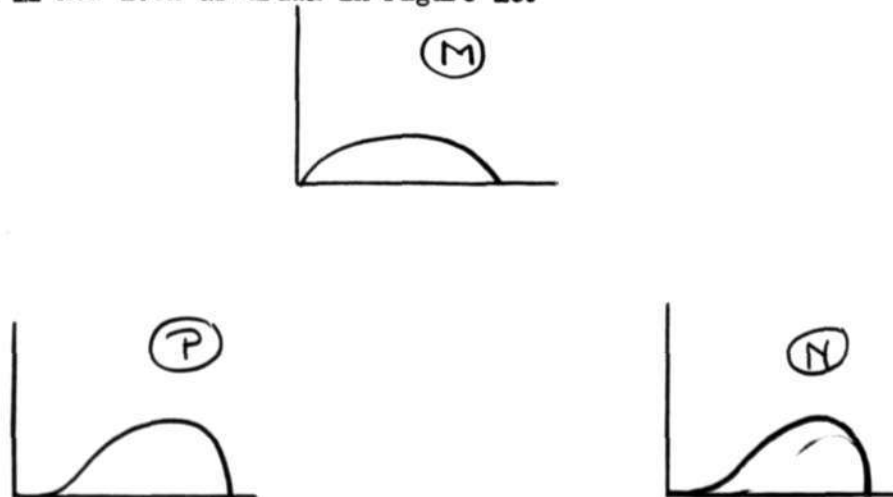



Figure 18: Magnetization curves for materials with  $\lambda = \mu$ , but  $\alpha \neq \beta$


The regions Q, R and V have vanished completely in transforming Figure 11 into Figure 17. Of the left-hand part of curve (N) the only portion

Memorandum M-2412

Page 30 of 30

remaining is the zero slope at absolute zero temperature. When  $\lambda = \mu$  the  $\alpha$ - $\beta$  map and the corresponding magnetization curves have become completely symmetrical about the line  $\alpha = \beta$ .

Signed   
Arthur E. Loeb

Approved   
David R. Brown

ALL/jk

cc: Group 63 Staff